

## Spin-3/2 Ising model for tricritical points in ternary fluid mixtures\*

S. Krinsky and D. Mukamel

*Department of Physics, Brookhaven National Laboratory, Upton, New York 11973*

(Received 15 July 1974)

We present a lattice-gas model of ternary fluid mixtures. Within the mean-field approximation, we study a nonsymmetric tricritical point in this model. We compare our results to the experimental observations on the system ethanol-water-carbon-dioxide. In the course of our work, we have studied a Landau theory describing the neighborhood of a fourth-order critical point. Also, we have noted that mean-field theory indicates the existence of a fourth-order critical point in the spin-1 model of Blume, Emery, and Griffiths, corresponding to  $K < 0$ ,  $J + K > 0$ .

### I. INTRODUCTION

We present an Ising spin- $\frac{3}{2}$  lattice-gas model of a ternary fluid mixture. Within the mean-field approximation, we study a nonsymmetric tricritical point in this model. A tricritical point can be defined as a point at which three phases simultaneously become identical. "Nonsymmetric" means that when the fields all have their tricritical values, the Hamiltonian has no special symmetry. This is in contrast to the symmetric tricritical points found in He<sup>3</sup>-He<sup>4</sup> mixtures, which were studied by Blume, Emery, and Griffiths.<sup>1</sup> A natural three-dimensional space in which to view the phase diagram in the neighborhood of a symmetric tricritical point is defined by choosing as variables the temperature  $T$ , a field  $\Delta$  which conserves the symmetry of the Hamiltonian, and a field  $H$  which breaks the symmetry. As noted by Griffiths,<sup>2</sup> the symmetric tricritical point is the terminus of three critical lines existing in the  $T, \Delta, H$  space (Fig. 1).

The natural space in which to exhibit the phase diagram in the neighborhood of a nonsymmetric tricritical point is four dimensional. Because the Hamiltonian has no special symmetry at the tricritical point, there does not exist a distinguished three-dimensional subspace. For a ternary fluid, one may choose the variables to be the temperature  $T$  and the chemical potentials  $\mu_1, \mu_2, \mu_3$  corresponding to the three types of constituent molecules. There exists a two-dimensional surface of critical points in the  $T, \mu_1, \mu_2, \mu_3$  space. The tricritical point is a special point on this surface, located at the intersection of two lines of critical end points (Fig. 2).

Using a one-order-parameter Landau expansion, Griffiths<sup>3</sup> has presented an enlightening discussion of the tricritical points in ternary fluid mixtures. We have extended the work of Griffiths, by relating the properties of the phase transition to the underlying molecular interactions. Of course, we have approximated the actual fluid by a simplified lattice gas, and we have studied the thermodynamics only within the mean-field approximation.

Stell and Hemmer<sup>4</sup> and Theumann and Hoye<sup>5</sup> have studied nonsymmetric tricritical points in certain one-dimensional systems with long-range Baker-Kac potentials. These models are interesting in their own right, but they are not easily interpretable as models of ternary fluid mixtures. Our spin- $\frac{3}{2}$  model can be straightforwardly compared with the results of experiments performed on ternary fluids. References to the experimental work can be found in the papers of Widom<sup>6</sup> and Griffiths.<sup>3</sup> We have (Sec. V) established a correspondence between the lattice-gas model and the system ethanol-water-carbon-dioxide studied by Shvarts and Efremova.<sup>7</sup>

Let us briefly describe our method of locating nonsymmetric tricritical points in the spin- $\frac{3}{2}$  model. The molecular interactions are parametrized by four interaction energies between molecules on nearest-neighbor sites. Consider the eight-dimensional space formed by the four interaction constants, the temperature, and the three chemical potentials. In this space, there exists a four-dimensional surface of symmetric tricritical points, which are joined to a four-dimensional surface of nonsymmetric tricritical points at a three-dimensional surface of symmetric fourth-order critical points. To find a nonsymmetric tricritical point, we have systematically searched in the neighborhood of a symmetric fourth-order critical point. After determining one typical tricritical point, we fixed the interaction energies and considered the temperature and the densities of the three components as variables. We have computed (Table II) the densities of the three components in the critical and coexisting noncritical phases for selected points on the critical end-point lines. Qualitative agreement is found with the system ethanol-water-carbon-dioxide.<sup>7</sup> However, the projections of the critical end-point lines onto the pressure-temperature plane for model and experiment have a qualitative difference. In the ethanol-water-carbon-dioxide system the tricritical point appears at the maximum temperature and pressure, while in

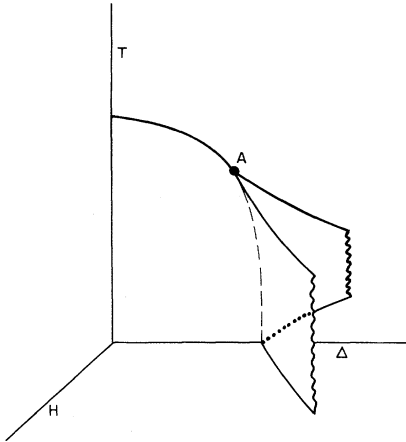


FIG. 1. Schematic phase diagram for  $\text{He}^3\text{-He}^4$  mixtures in the  $T, \Delta, H$  space.

the model it appears at the maximum temperature, but minimum pressure. Agreement with experiment may be possible by making an alternate choice of interaction energies. Choosing the interaction energies to optimize agreement between model and experiment remains for future work, as does study of the model away from the tricritical point.

The paper is organized as follows: In Sec. IIA we define the lattice-gas model; in Sec. IIB we develop the mean-field approximation; in Sec. IIC we derive equations determining the critical points; in Sec. IID we locate the symmetric tricritical and fourth-order critical points. In the course of our work, we noted that there exists in the Blume, Emery, Griffiths<sup>1</sup> model a symmetric fourth-order point corresponding to ferromagnetic exchange,  $J > 0$ , and negative biquadratic exchange,  $K < 0$ , with  $J + K > 0$ ; see Eq. (2.29). In Sec. III, we use a Landau expansion to study the neighborhood of a symmetric fourth-order critical point. Based upon the intuition gained from our study of the Landau theory, we locate, in Sec. IV, a nonsymmetric tricritical point in the spin- $\frac{3}{2}$  model. In Sec. V, we compare our model with the experimental system ethanol-water-carbon-dioxide.

## II. GENERAL FORMALISM

### A. Definition of model

We shall study the thermodynamics of a lattice-gas model of a ternary fluid mixture within the mean-field approximation. Our goal is to locate a nonsymmetric tricritical point, i. e., one such that the Hamiltonian has no special symmetry when the fields have their tricritical values. We shall denote the three types of molecules by 1, 2, and 3 and a vacancy by 0. The projection operators  $P^{(\lambda)}$  are defined by

$$P^{(\lambda)} P^{(\sigma)} = \delta_{\lambda\sigma} P^{(\lambda)} \quad (\lambda, \sigma = 0, 1, 2, 3), \quad (2.1a)$$

$$\sum_{\lambda=0}^3 P^{(\lambda)} = 1. \quad (2.1b)$$

The Kronecker  $\delta$  function is denoted  $\delta_{\lambda\sigma}$ . We consider a lattice having  $N$  sites, with each site possessing  $z$  nearest neighbors. The model Hamiltonian is

$$\begin{aligned} \mathcal{H} = & - \sum_{\langle ij \rangle} \sum_{\lambda=1}^3 \sum_{\sigma=1}^3 z^{-1} E_{\lambda\sigma} P_i^{(\lambda)} P_j^{(\sigma)} \\ & - \sum_{i=1}^N \sum_{\lambda=1}^3 \mu_{\lambda} P_i^{(\lambda)}. \end{aligned} \quad (2.2)$$

We use  $\langle ij \rangle$  to indicate that the sum is over nearest neighbors, and  $\mu_{\lambda}$  to denote the chemical potential of molecules of type  $\lambda = 1, 2, 3$ . The interaction energies are symmetric,

$$E_{\lambda\sigma} = E_{\sigma\lambda}, \quad (2.3a)$$

and vacancies are inert,

$$E_{0\lambda} = 0. \quad (2.3b)$$

The complexity of the mean-field calculation is kept within bounds by restricting our attention to interactions of the form

$$E_{\lambda\sigma} = E_0 + E_{\lambda} \delta_{\lambda\sigma} \quad (\lambda, \sigma = 1, 2, 3). \quad (2.3c)$$

When there are, for example, no type-2 molecules, the spin- $\frac{3}{2}$  Hamiltonian (2.2) becomes equivalent to the spin-1 Hamiltonian considered by Mukamel and Blume<sup>8</sup> ( $S_i = 1, 0, -1$ ),

$$\begin{aligned} \mathcal{H}_{\text{MB}} = & - \sum_{\langle ij \rangle} [J S_i S_j + K S_i^2 S_j^2 + C(S_i S_j^2 + S_i^2 S_j)] \\ & - \Delta \sum_{i=1}^N S_i^2 - H \sum_{i=1}^N S_i. \end{aligned} \quad (2.4)$$

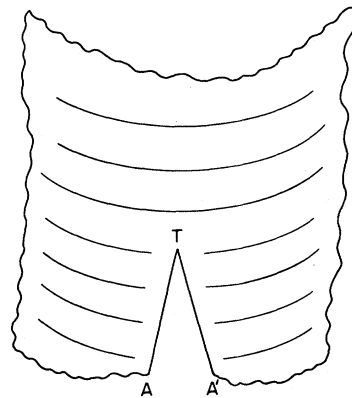


FIG. 2. Schematic drawing of the two-dimensional critical surface, existing in the four-dimensional phase space appropriate for ternary mixtures. Critical-end-point lines  $AT$  and  $A'T$  meet at the tricritical point  $T$ .

In the absence of type-2 molecules, the projection operators (2.1) can be expressed in terms of the spin-1 operators by  $P^{(0)} = 1 - S^2$ ,  $P^{(1)} = \frac{1}{2}(S^2 + S)$ ,  $P^{(2)} = 0$ ,  $P^{(3)} = \frac{1}{2}(S^2 - S)$ . The spin- $\frac{3}{2}$  Hamiltonian (2.2) is in that case equivalent to the spin-1 Hamiltonian (2.4) with

$$J = (E_1 + E_3)/4z, \quad (2.5a)$$

$$K = (E_1 + E_3 + 4E_0)/4z, \quad (2.5b)$$

$$C = (E_1 - E_3)/4z, \quad (2.5c)$$

$$H = \frac{1}{2}(\mu_1 - \mu_3), \quad (2.5d)$$

$$\Delta = \frac{1}{2}(\mu_1 + \mu_3). \quad (2.5e)$$

The conditions

$$E_\lambda + E_\sigma > 0 \quad (\lambda \neq \sigma = 0, 1, 2, 3), \quad (2.6)$$

are necessary and sufficient (Appendix A) to rule out staggered order at zero temperature for all values of the chemical potentials. In the following, we only consider interaction parameters satisfying (2.6) and we assume that there is no staggered ordering for nonzero temperatures. Therefore, when performing the mean-field calculations, we only consider translation-invariant states of the system.

The model specified by (2.2) and (2.3) differs from the spin- $\frac{3}{2}$  Ising model considered by Sivardière and Blume.<sup>9</sup> Their Hamiltonian contained dipolar and quadrupolar exchange, but no octupolar exchange. Hence there were interactions capable of driving critical fluctuations in only two of the three possible order parameters. Also, they considered only symmetric exchange interactions. Our Hamiltonian possesses interactions coupling to all three order parameters, and also contains nonsymmetric interactions. In fact, the model considered by Sivardière and Blume is not a special case of our model, since the interactions cannot be parametrized in the form (2.3).

### B. Mean-field approximation

We derive the mean-field approximation by using the variational principle<sup>10</sup> for the free energy

$$F \leq N\phi \equiv \text{Tr}(\rho\beta\mathcal{C}) + \beta^{-1} \text{Tr}(\rho \ln \rho), \quad (2.7)$$

where  $F$  is the exact free energy and  $\rho$  is any trial density matrix. To obtain the mean-field approximation, we assume

$$\rho = \prod_{i=1}^N \rho_i, \quad (2.8)$$

where  $\rho_i$  is a density matrix defined on the single site  $i$ . For a translationally invariant system, we can write

$$\rho_i = \sum_{\lambda=0}^3 A_\lambda P_i^{(\lambda)}, \quad (2.9a)$$

where

$$\text{Tr} \rho_i = A_1 + A_2 + A_3 + A_0 = 1. \quad (2.9b)$$

Then, the density  $A_\lambda$  is given by

$$A_\lambda = \text{Tr}(\rho P_i^{(\lambda)}) \quad (\lambda = 0, 1, 2, 3). \quad (2.10)$$

Using (2.7) together with (2.2) and (2.3) we find

$$\begin{aligned} \phi = & -\frac{1}{2} E_0 (A_1 + A_2 + A_3)^2 - \sum_{\lambda=1}^3 \left( \frac{1}{2} E_\lambda A_\lambda^2 + \mu_\lambda A_\lambda \right) \\ & + \beta^{-1} \sum_{\lambda=0}^3 A_\lambda \ln A_\lambda. \end{aligned} \quad (2.11)$$

The best approximation to the free energy is determined by choosing  $A_1$ ,  $A_2$ , and  $A_3$  to minimize the right-hand side of (2.11). The local minima of  $\phi$  are determined by  $\partial\phi/\partial A_\lambda = 0$  ( $\lambda = 1, 2, 3$ ) together with the condition that  $\partial^2\phi/\partial A_\lambda \partial A_\sigma$  be a positive definite matrix. If for a given set of fields there are several local minima, it is necessary to select the one corresponding to the smallest value of  $\phi$ . If  $\partial^2\phi/\partial A_\lambda \partial A_\sigma$  has a zero eigenvalue, it is necessary to consider higher derivatives to determine stability. When there is stability, the existence of a zero eigenvalue corresponds to criticality.

The equations  $\partial\phi/\partial A_\lambda = 0$  ( $\lambda = 1, 2, 3$ ) relate the densities  $A_\lambda$  to the fields  $\mu_\lambda$ . Using (2.11), we find

$$\mu_1 = -E_0(A_1 + A_2 + A_3) - E_1 A_1 + \beta^{-1} \ln(A_1/A_0), \quad (2.12a)$$

$$\mu_2 = -E_0(A_1 + A_2 + A_3) - E_2 A_2 + \beta^{-1} \ln(A_2/A_0), \quad (2.12b)$$

$$\mu_3 = -E_0(A_1 + A_2 + A_3) - E_3 A_3 + \beta^{-1} \ln(A_3/A_0). \quad (2.12c)$$

In Appendix B, we show how these three equations can be reduced to one equation, suitable for numerical solution. The second-derivative matrix is

$$\frac{\partial^2\phi}{\partial A_\lambda \partial A_\sigma} = \begin{pmatrix} \alpha_0 + \alpha_1 & \alpha_0 & \alpha_0 \\ \alpha_0 & \alpha_0 + \alpha_2 & \alpha_0 \\ \alpha_0 & \alpha_0 & \alpha_0 + \alpha_3 \end{pmatrix}, \quad (2.13)$$

where we define

$$\alpha_\lambda = -E_\lambda + (\beta A_\lambda)^{-1} \quad (\lambda = 0, 1, 2, 3). \quad (2.14)$$

The determinant of (2.13) is given by

$$\begin{aligned} \det \left( \frac{\partial^2\phi}{\partial A_\lambda \partial A_\sigma} \right) = & \alpha_0 \alpha_1 \alpha_2 + \alpha_0 \alpha_2 \alpha_3 \\ & + \alpha_0 \alpha_3 \alpha_1 + \alpha_1 \alpha_2 \alpha_3. \end{aligned} \quad (2.15)$$

## C. Determination of critical points

Suppose the determinant (2.15) has a *simple*<sup>11</sup> zero for the critical values of the densities  $A = (A_1, A_2, A_3)$ . A special direction in the density space is defined by the eigenvector  $Z = (Z_1, Z_2, Z_3)$  of the second-derivative matrix (2.13) corresponding to the zero eigenvalue. Consider deviations in the density space from the point  $A$  in the direction  $Z$ , measured by the small parameter  $\Psi$ , i. e.,

$$(\bar{A}_1, \bar{A}_2, \bar{A}_3) = (A_1, A_2, A_3) + (Z_1, Z_2, Z_3)\Psi. \quad (2.16)$$

An expansion analogous to a Landau expansion in the one-order parameter  $\Psi$  is given by

$$\phi(\bar{A}) = \phi(A) + \sum_{n=3}^{\infty} \frac{\Psi^n C_n(A)}{n!}, \quad (2.17a)$$

where

$$C_n(A) = \sum_{\lambda_1, \dots, \lambda_n=1}^3 \left( \frac{\partial^n \phi}{\partial A_{\lambda_1} \dots \partial A_{\lambda_n}} \right) Z_{\lambda_1} \dots Z_{\lambda_n}. \quad (2.17b)$$

For  $n \geq 3$ , we find

$$C_n(A) = \beta^{-1}(n-2)! \times \left( A_0^{1-n} (Z_1 + Z_2 + Z_3)^n + \sum_{\lambda=1}^3 A_{\lambda}^{1-n} (-Z_{\lambda})^n \right). \quad (2.17c)$$

Note that the expansion (2.17a) of  $\phi$  about the critical point begins with the  $\Psi^3$  term. The extremal conditions  $\partial\phi/\partial A_{\lambda} = 0$  ( $\lambda = 1, 2, 3$ ) imply the term linear in  $\Psi$  vanishes. At criticality,  $\det(\partial^2\phi/\partial A_{\lambda}\partial A_{\mu}) = 0$ . We chose  $Z$  to be the eigenvector of the Jacobian matrix corresponding to the zero eigenvalue, so

$$\sum_{\lambda} \left( \frac{\partial^2 \phi}{\partial A_{\mu} \partial A_{\lambda}} \right) Z_{\lambda} = 0 \quad (\mu = 1, 2, 3),$$

showing that the term quadratic in  $\Psi$  vanishes. A necessary condition for a stable critical point is that  $C_3$  vanish, otherwise, instead of a minimum one has a saddle point.

There are two classes of critical points corresponding to the vanishing of determinant (2.15). The first class corresponds to vanishing of two of the alphas. To be specific, we shall consider

$$\alpha_1 = \alpha_3 = 0, \quad (2.18)$$

with

$$\alpha_0 > 0, \quad \alpha_2 > 0. \quad (2.19)$$

The eigenvector corresponding to the zero eigenvalue of (2.13) is  $Z = (1, 0, -1)$ , hence  $C_3 = (\beta A_1^2)^{-1}$

$-(\beta A_1^2)^{-1}$ . Therefore (2.18) together with  $C_3 = 0$  implies

$$E_1 = E_3 \equiv E, \quad (2.20a)$$

$$A_1 = A_3 = 1/\beta E. \quad (2.20b)$$

These critical points are symmetric, since the Hamiltonian with the fields having their critical values is invariant under the exchange of type-1 and type-3 molecules. It is easy to verify that (2.19) is a necessary and sufficient condition for the positivity of the two nonzero eigenvalues of (2.13).

The determinant (2.15) also vanishes when

$$\alpha_0^{-1} + \alpha_1^{-1} + \alpha_2^{-1} + \alpha_3^{-1} = 0. \quad (2.21)$$

The second class of critical points, corresponding to (2.21), will be nonsymmetric. Let us rewrite (2.21) in the form

$$\frac{A_0}{1 - \beta E_0 A_0} + \frac{A_1}{1 - \beta E_1 A_1} + \frac{A_2}{1 - \beta E_2 A_2} + \frac{A_3}{1 - \beta E_3 A_3} = 0. \quad (2.22a)$$

Since the eigenvector of (2.13) corresponding to the zero eigenvalue is  $Z = (\alpha_1^{-1}, \alpha_2^{-1}, \alpha_3^{-1})$ , we see from (2.17) that the condition  $C_3 = 0$  is

$$\frac{A_0}{(1 - \beta E_0 A_0)^3} + \frac{A_1}{(1 - \beta E_1 A_1)^3} + \frac{A_2}{(1 - \beta E_2 A_2)^3} + \frac{A_3}{(1 - \beta E_3 A_3)^3} = 0. \quad (2.22b)$$

Equations (2.22) are necessary conditions which must be satisfied by the nonsymmetric critical points. The two nonzero eigenvalues of (2.13) are again positive if  $\alpha_0 > 0$  and  $\alpha_2 > 0$ .

Some of the symmetric critical points given in (2.20) are tricritical. Let us derive a necessary condition which must be satisfied by those that are tricritical. We generalize the form of the deviations considered in (2.16), letting

$$(\bar{A}_1, \bar{A}_2, \bar{A}_3) = (A_1, A_2, A_3) + (1, 0, -1)\Psi + (u, v, u)\Psi^2.$$

Then the analogue of a Landau expansion becomes

$$\phi(\bar{A}) = \phi(A) + R\Psi^4 + O(\Psi^6),$$

where

$$R = \frac{1}{2} \alpha_0 (2u + v)^2 + \frac{1}{2} \alpha_2 v^2 - \beta E^2 u + \frac{1}{6} \beta^2 E^3.$$

We choose  $u$  and  $v$  so as to minimize  $R$ , and we find ( $\alpha_0 > 0$  and  $\alpha_2 > 0$ )

$$R_{\min} = -\frac{1}{8} \beta^2 E^4 (1/\alpha_0 + 1/\alpha_2) + \frac{1}{6} \beta^2 E^3.$$

A necessary condition for tricriticality is  $R_{\min} = 0$ , i. e.,

$$\frac{4}{3} (\beta E)^{-1} = \frac{A_0}{1 - \beta E_0 A_0} + \frac{A_2}{1 - \beta E_2 A_2}. \quad (2.23)$$

## D. Symmetric tricritical points

Let us consider the special case  $E_1 = E_3$  and locate the symmetric tricritical and fourth-order critical points. In order to make clear the relationship of our work to that of Blume, Emery, and Griffiths<sup>1</sup> on the spin-1 Ising model of He<sup>3</sup>-He<sup>4</sup> mixtures, we define

$$2J \equiv E_1 = E_3, \quad K \equiv E_0 + J,$$

$$2H \equiv \mu_1 - \mu_3, \quad M \equiv A_1 - A_3,$$

$$2\Delta \equiv \mu_1 + \mu_3, \quad Q \equiv A_1 + A_3.$$

Equations (2.12) become

$$H = -JM + \frac{1}{2\beta} \ln \frac{Q+M}{Q-M}, \quad (2.24a)$$

$$\Delta = -KQ - E_0 A_2 + \frac{1}{2\beta} \ln \frac{Q^2 - M^2}{4(1-Q-A_2)^2}, \quad (2.24b)$$

$$\mu_2 = -E_0(Q+A_2) - E_2 A_2 + \frac{1}{\beta} \ln \frac{A_2}{1-Q-A_2}. \quad (2.24c)$$

As is expected from (2.5), in the limit  $A_2 \rightarrow 0$  these equations reduce to those of Blume, Emery, and Griffiths.<sup>1</sup> In their model,  $M = \langle S_i \rangle$  denotes the superfluid order parameter and  $x = 1 - Q = 1 - \langle S_i^2 \rangle$  denotes the concentration of He<sup>3</sup>.

It is straightforward to determine  $H$  as a series in powers of  $M$ ,

$$H = 2aM + 4bM^3 + 6cM^5 + 8dM^7 + \dots \quad (2.25)$$

The coefficients  $a$ ,  $b$ ,  $c$ , and  $d$  are functions of the fields  $\Delta$ ,  $\mu_2$ ,  $E_\lambda$ , and  $\beta$ . These coefficients are most easily expressed in terms of  $A_2$  and  $\bar{Q}$ , which are implicitly defined as functions of the fields by

$$\Delta = -E_0(\bar{Q} + \bar{A}_2) - J\bar{Q} + \frac{1}{\beta} \ln \frac{\bar{Q}}{2(1-\bar{Q}-\bar{A}_2)}, \quad (2.26a)$$

$$\mu_2 = -E_0(\bar{Q} + \bar{A}_2) - E_2 \bar{A}_2 + \frac{1}{\beta} \ln \frac{\bar{A}_2}{1-\bar{Q}+\bar{A}_2}. \quad (2.26b)$$

When  $M=0$ ,  $\bar{A}_2 = A_2$  and  $\bar{Q} = Q$ , we find

$$2a = -J + (\beta\bar{Q})^{-1}. \quad (2.27a)$$

The symmetric critical points are determined by  $a=0$  and  $b>0$ . The constraint (2.19) assures that this specifies a local minimum of  $\phi$ , and not a saddle point. When  $a=0$  (i. e.,  $\bar{Q} = 1/\beta J$ ),

$$b = \frac{1}{8\beta\bar{Q}^4} \left( \frac{2\bar{Q}}{3} - \frac{\bar{A}_2}{1-\beta E_2 \bar{A}_2} - \frac{\bar{A}_0}{1-\beta E_0 \bar{A}_0} \right). \quad (2.27b)$$

where  $\bar{A}_0 = 1 - \bar{Q} - \bar{A}_2$ . The symmetric tricritical points are determined by  $a=b=0$ ,  $c>0$ . The con-

dition  $a=b=0$  is equivalent to (2.23), derived in the previous section. When  $a=b=0$ ,

$$c = \frac{1}{48\beta\bar{Q}^6} \left( -\frac{4\bar{Q}}{135} + \frac{\bar{A}_2}{(1-\beta E_2 \bar{A}_2)^3} + \frac{\bar{A}_0}{(1-\beta E_0 \bar{A}_0)^3} \right). \quad (2.27c)$$

Since  $M=0$ , it follows that  $\bar{A}_2 = A_2$  and  $\bar{Q} = Q$  at the symmetric critical and tricritical points. Therefore Eqs. (2.27) can be directly used to determine the position of the symmetric tricritical points. The fourth-order critical points are given by  $a=b=c=0$ ,  $d>0$ .

The nonsymmetric critical lines which meet the symmetric critical line at a tricritical point can be determined by solving numerically Eqs. (2.22).

As an explicit example, consider  $E_1 = E_3 = 1$ ,  $E_0 = 1.2$ ,  $E_2 = -0.62$ ,  $\beta = 9.0$ . In Fig. 3(a), we plot the critical lines in the neighborhood of the symmetric tricritical point located at  $A_1 = A_3 = \beta^{-1}$ ,  $A_2 = 0.77526$ . In Fig. 3(b), we consider the case of  $E_1 \neq E_3$ . In particular, we exhibit the critical lines when

$$E_1 = 1 + e, \quad (2.28a)$$

$$E_3 = 1 - e, \quad (2.28b)$$

with  $e = 10^{-5}$ . The critical lines do not intersect, and there does not exist a nonsymmetric tricritical point in the neighborhood of the symmetric tricritical point. The critical line corresponding to  $M < 0$  terminates in a critical end point. As  $e \rightarrow 0$ , the critical end point approaches the symmetric tricritical point.

Just as the neighborhood of a symmetric tricritical point is a good place to look for nonsymmetric critical lines, the neighborhood of a fourth-order critical point is where to find nonsymmetric tricritical points. Before continuing our discussion of the spin- $\frac{3}{2}$  model, let us point out that there exists a fourth-order critical point in the spin-1 model (2.4) considered by Blume, Emery, and Griffiths<sup>1</sup> ( $C=0$ ) and Mukamel and Blume<sup>8</sup> ( $C \neq 0$ ). They considered only positive biquadratic exchange  $K > 0$ . The fourth-order critical point exists for  $K < 0$  and  $J+K > 0$ . Since  $J+K > 0$ , there is no staggered order at zero temperature for any values of the magnetic and crystal fields. Within the mean-field approximation, considering only translation-invariant states, a stable fourth-order critical point is located at

$$Q = 1/(1 + \sqrt{10}), \quad (2.29a)$$

$$\beta J Q = 1, \quad (2.29b)$$

$$2\beta K Q = (3Q - 1)/(1 - Q), \quad (2.29c)$$

$$C = H = 0. \quad (2.29d)$$

There exist nonsymmetric tricritical points in the neighborhood of (2.29) with  $C \neq 0$ .

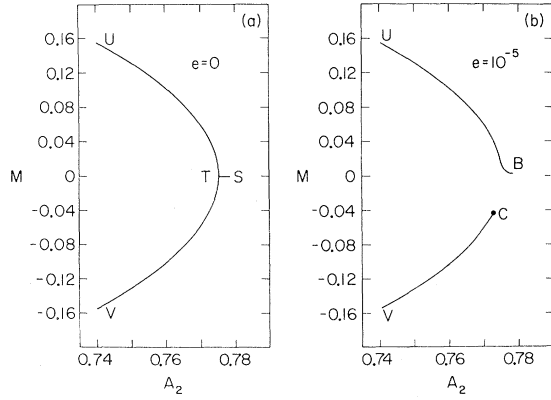


FIG. 3. Projection of a portion ( $A_2 \geq 0.74$ ) of the critical lines onto  $M, A_2$  plane. When (a)  $e=0$ , nonsymmetric lines  $UT$  and  $VT$  meet symmetric line  $TS$  at symmetric tricritical point  $T$ . When (b)  $e=10^{-5}$ , the line  $VC$  terminates in critical end point  $C$ . The points  $S$  in (a) and  $B$  in (b) correspond to  $A_1 + A_2 + A_3 = 1$ .

In Sec. IV, we find a fourth-order critical point in the spin- $\frac{3}{2}$  model, and we locate a nonsymmetric tricritical point. But first, in Sec. III, we present a qualitative description of the neighborhood of a fourth-order critical point using a Landau expansion. The Landau theory is very useful for developing the intuition necessary to find a nonsymmetric tricritical point in the spin- $\frac{3}{2}$  model.

### III. LANDAU MODEL FOR A FOURTH-ORDER CRITICAL POINT

In this section, we use a Landau model to discuss the phase diagram near a fourth-order critical point. In particular, we are interested in the topology of the critical and coexistence surfaces near that point. We start by assuming that the system can be described by a one-dimensional order parameter  $\Psi$ , which for multicomponent fluid mixtures is some linear combination of the densities of the various components in the system. In the Landau model, one assumes that the appropriate free energy  $F$  can be expanded in a power series in  $\Psi$ . For describing fourth-order critical points, it is sufficient to consider this expansion up to eighth order in  $\Psi$ ,

$$F[a_i; \Psi] = \sum_{i=0}^8 a_i \Psi^i. \quad (3.1)$$

To maintain stability,  $a_8$  should be positive, and without loss of generality, one can assume that  $a_8 = 1$ . The coefficients  $a_i$  are functions of the physical fields which appear in the Hamiltonian of the system. Following Landau,<sup>12</sup> we assume that the coefficients are analytic functions. One can therefore expand the  $a_i$  in power series in the physical fields, and consider the expansion up to first or-

der near the fourth-order critical point. The fact that the  $a_i$  are related to the physical fields by a linear transformation implies that the topology of the phase diagram near the fourth-order critical point should be the same in the  $a_i$  space and the space of the physical fields. We shall therefore consider the phase diagram corresponding to the free energy (3.1) in the  $a_i$  space. This phase diagram is obtained by studying the minima of the free energy. The equilibrium free energy is given by the concave function

$$\bar{F} = \min_{\Psi} F[a_i; \Psi].$$

To study the minima, it is more convenient to rewrite the free energy (3.1) in the form

$$F = F_0 + (\Psi - \Psi_1)^2 [(\Psi - \Psi_2)^2 + R_2^2] [(\Psi - \Psi_3)^2 + R_3^2] \times [(\Psi - \Psi_4)^2 + R_4^2], \quad (3.2)$$

where  $F_0$ ,  $\Psi_i$ , and  $R_j$  are parameters which are related to the  $a_i$  in a straightforward way. The phase diagram corresponding to this free energy in the  $(\Psi_i, R_j)$  space is summarized in Table I, where we assume that  $\Psi_1 = 0$ . To obtain the phase diagram in the  $a_i$  space, one can use Eq. (3.2) to express the  $a_i$  in terms of  $\Psi_i$  and  $R_j$ . This provides us with a parametric representation of the various critical and coexistence surfaces in the  $a_i$  space. The critical and tricritical surfaces can also be found directly by solving the equations

$$\frac{\partial^n F}{\partial \Psi^n} = 0, \quad n = 1, 2, 3, \quad \frac{\partial^4 F}{\partial \Psi^4} > 0, \quad (3.3)$$

for critical points, and

$$\frac{\partial^n F}{\partial \Psi^n} = 0, \quad n = 1, \dots, 5, \quad \frac{\partial^6 F}{\partial \Psi^6} > 0, \quad (3.4)$$

for tricritical points.

Let us now consider the coefficients of the Landau expansion to be related to the fields in the spin- $\frac{3}{2}$  model. For  $E_1 = E_3$ , we derived in (2.25), (2.26), and (2.27) an expansion of  $H \equiv \frac{1}{2}(\mu_1 - \mu_3)$  in powers of  $M \equiv A_1 - A_3$ , which is of the Landau form (3.1), with  $a_3 = a_5 = a_7 = 0$ . For  $e \equiv E_1 - E_3 \neq 0$ , the analogous Landau expansion would have nonzero  $a_3$ ,  $a_5$ , and  $a_7$ , with  $a_3$ ,  $a_5$ , and  $a_7$  all proportional to  $e$ , as  $e \rightarrow 0$ . The general features of the phase diagram of the spin- $\frac{3}{2}$  model can be understood by studying the Landau expansion with  $a_5 = a_7 = 0$ , but  $a_3 \neq 0$ . Let

$$F = -\hbar\Psi + a\Psi^2 + \epsilon\Psi^3 + b\Psi^4 + c\Psi^6 + \Psi^8. \quad (3.5)$$

Since we are relating the coefficients in this expansion to the fields of the spin- $\frac{3}{2}$  model, we can distinguish between "symmetric" and "nonsymmetric" critical points on the basis of whether or not the Hamiltonian is symmetric at the critical values of the fields. Then, we see that a symmet-

TABLE I. Critical and coexistence surfaces near a fourth-order critical point.

No.	Type of surface	Equations	Dimension
1	Fourth-order critical point	$\Psi_i = 0, R_i = 0, i = 2, 3, 4$	0
2	Tricritical end points	$\Psi_2 = \Psi_3 = 0, R_i = 0, i = 2, 3, 4$	1
3	Two coexisting critical points	$\Psi_2 = 0, \Psi_2 = \Psi_4, R_i = 0, i = 2, 3, 4$	1
4	Critical point coexisting with two phases	$\Psi_2 = 0, R_i = 0, i = 2, 3, 4$	2
5	Tricritical points	$\Psi_2 = \Psi_3 = 0, R_2 = R_3 = 0$	2
6	Critical end points	$\Psi_2 = 0, R_2 = R_3 = 0$	3
7	Four coexisting phases	$R_i = 0, i = 2, 3, 4$	3
8	Critical points	$\Psi_2 = 0, R_2 = 0$	4
9	Triple points	$R_2 = R_3 = 0$	4
10	Two coexisting phases	$R_2 = 0$	5

ric fourth-order critical point is located at

$$h = \epsilon = a = b = c = 0, \quad \Psi = 0. \quad (3.6)$$

The symmetric tricritical points correspond to

$$h = \epsilon = a = b = 0, \quad c > 0, \quad \Psi = 0. \quad (3.7a)$$

Two lines of nonsymmetric tricritical points are specified by

$$a = -15\left(\frac{3}{28}\right)^3 c^3, \quad b = \frac{45}{56} c^2, \quad \epsilon = \pm \frac{9}{49} \sqrt{\frac{28}{3}} |c|^{5/2},$$

$$h = \mp \left(\frac{3}{7}\right)^3 \sqrt{\frac{3}{28}} |c|^{7/2}, \quad \Psi = \mp \sqrt{\frac{3}{28}} |c|^{1/2}, \quad c < 0. \quad (3.7b)$$

The symmetric critical points correspond to

$$h = \epsilon = a = 0, \quad b > 0, \quad \Psi = 0, \quad (3.8a)$$

and the nonsymmetric critical points to

$$a = -\frac{3}{2} \epsilon \Psi + 15c\Psi^4 + 56\Psi^6,$$

$$b = -\frac{1}{4} \epsilon \Psi^{-1} - 5c\Psi^2 - 14\Psi^4, \quad (3.8b)$$

$$h = -\epsilon \Psi^2 + 16c\Psi^5 + 64\Psi^7.$$

The solutions (3.7) and (3.8) of Eqs. (3.4) and (3.3), respectively, include unstable critical points, for which the order parameter  $\Psi$  at the critical point does not correspond to the absolute minimum of the free energy. The stability of the solutions must therefore be checked separately.

Let us discuss now the phase diagram and consider first the case  $\epsilon = 0$ . The phase diagram (for  $c = 1$ ) in the  $a$ - $b$  plane ( $h = 0$ ) is given in Fig. 4(a) and the projections of the critical and triple point lines on the  $a$ - $h$  plane are given in Fig. 4(b). The analogous diagrams for  $c = -1$  are given in Figs. 4(c) and 4(d). For  $c = +1$ , one obtains the usual symmetric tricritical point  $T$ . For  $c = -1$ , there exists no tricritical point. The point  $A$  (which corresponds to  $\Psi_1 = \Psi_2 = -\Psi_3 = -\Psi_4, R_i = 0$ , and  $i = 2, 3, 4$  in the  $\Psi_i - R_i$  representation) is a point where

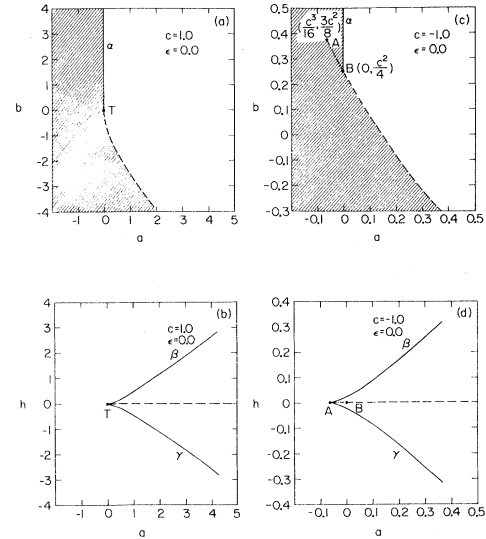


FIG. 4. Phase diagram corresponding to the free energy (3.5) for  $\epsilon = 0$ . Solid lines: critical lines; dashed lines: triple-point lines; dashed-dotted lines: coexistence lines of four phases. (a) Phase diagram for  $c = +1$  in the  $a$ - $b$  plane.  $\alpha$  is a symmetric critical line and  $T$  is a symmetric tricritical point. Shaded part of the plane is a coexistence surface of two phases. (b) Projection of the critical- and triple-point lines on the  $a$ - $h$  plane, for  $c = +1$ .  $\beta$  and  $\gamma$  are nonsymmetric critical lines. The critical line  $\alpha$  of Fig. 4(a) is projected on the symmetric tricritical point  $T$ . (c) Phase diagram in the  $a$ - $b$  plane for  $c = -1$ .  $\alpha$  is a symmetric critical line,  $A$  is a point where two critical phases coexist, and  $B$  is a critical end point coexisting with two other phases. The shaded part of the plane is a coexistence surface of two phases. A schematic form of the phase diagram in the  $a$ - $b$ - $h$  space is given in Fig. 5(a). (d) A projection (for  $c = -1$ ) of the critical lines, triple-point lines, and lines of coexistence of four phases on the  $a$ - $h$  plane.  $\beta$  and  $\gamma$  are nonsymmetric critical lines. The symmetric critical line,  $\alpha$ , of Fig. 4(c) is projected on the point  $B$ .

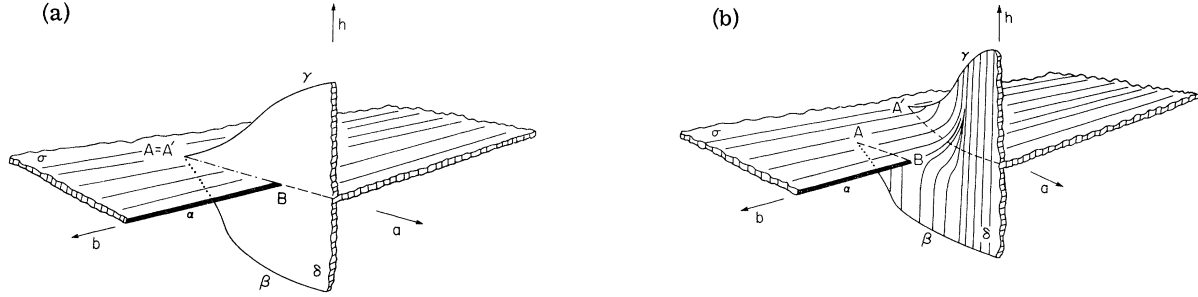


FIG. 5. Schematic form of the phase diagram corresponding to the free energy (3.5) ( $c = -1$ ), in the  $a$ - $b$ - $h$  space. (a)  $\epsilon = 0$ . Here,  $\delta$  and  $\sigma$  are coexistence surfaces of two phases. The surface  $\delta$  is bounded by two nonsymmetric critical lines  $\beta$  and  $\gamma$ , and the surface  $\sigma$  is bounded by a symmetric critical line  $\alpha$  and a triple-point line (the dashed line). The point  $A$  corresponds to the coexistence of two critical phases, and  $B$  is a critical end point coexisting with two other phases.  $A$  and  $B$  are connected by a coexistence line of four phases (the dashed-dotted line). As  $c$  goes to zero, the points  $A$  and  $B$  approach each other and they coincide for  $c = 0$ , forming a fourth-order critical point. For positive  $c$ , they become a symmetric tricritical point. In this case, the phase diagram is described by the projections in Figs. 4(a) and 4(b). (b)  $\epsilon > 0$ . Here,  $\alpha$ ,  $\beta$ , and  $\gamma$  are nonsymmetric critical lines.  $A$  and  $B$  are critical end points. The upper and lower parts of the coexistence surface  $\delta$  split into two different surfaces near the point  $B$ . The coexistence line of four phases [of Fig. 5(a)] splits into two triple-point lines. As  $\epsilon$  is increased, the two critical end points  $A$  and  $B$  approach each other, and they coincide for  $\epsilon = 0.56$ , forming a nonsymmetric tricritical point. For  $\epsilon > 0.56$ , the critical end points  $A$  and  $B$  no longer exist, and the two critical lines  $\alpha$  and  $\beta$  form one continuous nonsymmetric critical line.

two critical phases coexist. The point  $B$  (which corresponds to  $\Psi_1 = \Psi_2 = 0$ ,  $\Psi_3 = -\Psi_4$ ,  $R_i = 0$ , and  $i = 2, 3, 4$  in the  $\Psi_i - R_i$  representation) is a critical end point coexisting with two noncritical phases. The points  $A$  and  $B$  are connected by a line of four coexisting phases. A schematic form of the phase diagram, for  $c = -1$  and  $\epsilon = 0$ , in the  $a$ - $b$ - $h$  space is given in Fig. 5(a). As  $c$  goes to zero, the points  $A$  and  $B$  become closer, and at  $c = 0$  they coincide, forming a fourth-order critical point. For  $c > 0$  this point becomes a symmetric tricritical point, where  $\alpha$  is the symmetric critical line and  $\beta$ ,  $\gamma$  are the nonsymmetric critical lines [compare with Figs. 4(a) and 4(b)]. The phase diagram for a nonzero  $\epsilon$  and positive  $c$  was discussed in detail by Griffiths<sup>3</sup> and Schulman.<sup>13</sup> In this region there are no tricritical points, and we shall not repeat the discussion here. The phase diagram in the  $a$ - $b$ - $h$  space, for small positive  $\epsilon$  and  $c = -1$ , is described schematically in Fig. 5(b). In this case the line of four coexisting phases [of Fig. 5(a)] splits into two lines of triple points, the point  $A$  splits into two critical end points  $A$  and  $A'$ , and  $B$  becomes a critical end point. As  $\epsilon$  is increased, the two points  $A$  and  $B$  become closer, and they coincide for  $\epsilon = \frac{9}{49} \sqrt{\frac{20}{3}} |c|^{5/2}$ , forming a nonsymmetric tricritical point. The projections of the critical- and triple-point lines on the  $a$ - $b$  plane, for several values of  $\epsilon$ , are given in Fig. 6.

In solving Eqs. (3.3) for the critical points, one finds that there are two continuous lines of solutions for  $\epsilon \neq 0$  and  $c$  fixed. One line is  $\gamma$ , and the other is a line which consists of the stable segments  $\alpha$  and  $\beta$ , connected by an unstable segment between the critical end points  $A$  and  $B$ , [Fig. 5(b)].

The unstable part is not shown in the figure. As  $\epsilon$  is increased towards its tricritical value [Eq. (3.7b)], the unstable part shrinks to a point, so the critical end points  $A$  and  $B$  approach one another and meet at the nonsymmetric tricritical point. Therefore, in looking for a nonsymmetric tricritical point in the spin- $\frac{3}{2}$  model, we do not look for an intersection of two lines of solutions of the critical equations (2.22) (as one usually does when looking for a symmetric tricritical point), but rather we look for the approach of two critical end points located on one line of solutions to Eqs. (2.22). The point where they meet is the nonsymmetric tricritical point. This procedure is described in detail in Sec. IV.

#### IV. DETERMINATION OF A NONSYMMETRIC TRICRITICAL POINT

We are now ready to find, within the mean-field approximation, a nonsymmetric tricritical point in the spin- $\frac{3}{2}$  model. To begin, we consider the expansion (2.25) of  $H \equiv \frac{1}{2}(\mu_1 - \mu_3)$  in powers of  $M \equiv A_1 - A_3$ . The symmetric tricritical points are characterized by  $a = b = 0$ ,  $c > 0$ , and the fourth-order critical points by  $a = b = c = 0$ ,  $d > 0$ . There are eight independent variables in the spin- $\frac{3}{2}$  model, and they can be chosen to be  $\beta$ ,  $E_0$ ,  $E_1$ ,  $E_2$ ,  $E_3$ ,  $A_1$ ,  $A_2$ , and  $A_3$ . These are related to the coefficients of (2.25) by (2.27). In the eight-dimensional parameter space there exists a four-dimensional surface of symmetric tricritical points. This surface joins a four-dimensional surface of nonsymmetric tricritical points at a three-dimensional surface of fourth-order critical points. Since our goal is to determine one nonsymmetric tricritical



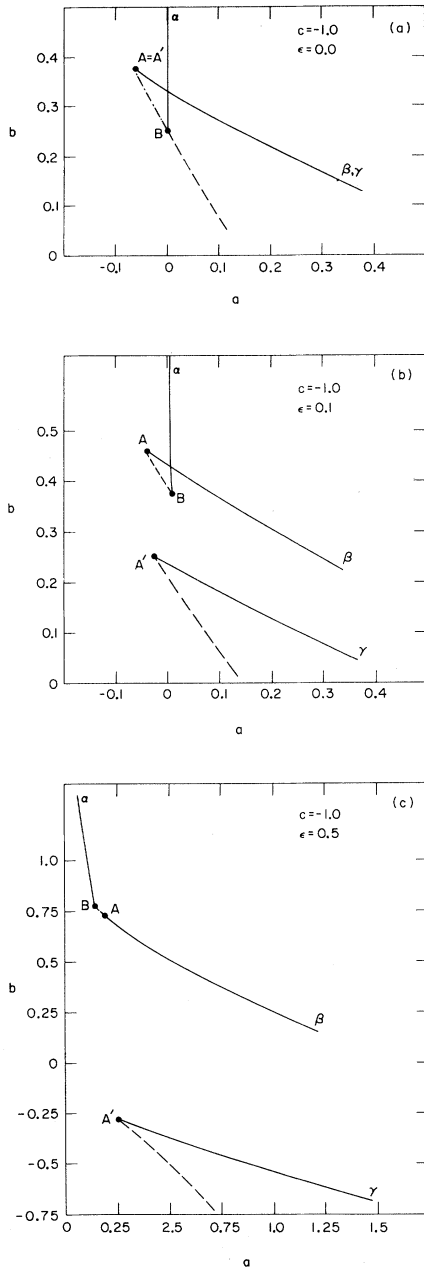


FIG. 6. Projection of the critical- and triple-point lines on the  $a$ - $b$  plane (for  $c = -1$ ) and several values of  $\epsilon$ . As  $\epsilon$  is increased from zero, the two critical end points  $A$ ,  $B$  approach each other, and will meet at the nonsymmetric tricritical point for  $\epsilon = 0.56$ .

point, we are free to fix several variables at our convenience. We choose

$$\beta = 9, E_0 = 1.2, E_1 = 1 + e, E_3 = 1 - e,$$

where  $e$  will play the role of a symmetry-breaking parameter.

First, we consider  $e = 0$ . For  $E_2 = -0.62$ , there

exists a symmetric tricritical point at  $A_1 = A_3 = \beta^{-1}$ ,  $A_2 = 0.77526$ , as was noted in Sec. IID. The critical lines meeting at the tricritical point were shown in Fig. 3(a). By varying  $E_2$ , one sweeps out a line of symmetric tricritical points. When  $E_2 = -0.613523$ , the line terminates in a fourth-order critical point, located at  $A_1 = A_3 = \beta^{-1}$ ,  $A_2 = 0.77650$ . To find a nonsymmetric tricritical point near the fourth-order point, we should increase  $E_2$  past its fourth-order value, so that there exists an "unstable tricritical point" with  $a = b = 0$ ,  $c < 0$ , and  $d > 0$ . A suitable choice is

$$E_2 = -0.613.$$

Our motivation lies in the discussion of the Landau theory presented in Sec. III.

For  $e = 0$  and  $E_2 = -0.613$ , we draw the projection of the critical lines onto the  $M, A_2$  plane in Fig. 7(a). The two nonsymmetric critical lines do not intersect. They each terminate in a critical end point, denoted  $A$  and  $A'$ , respectively. These critical end points correspond to  $H = 0$ , and non-zero magnetizations of equal magnitude, but of opposite sign. Usually, a critical end point corresponds to a critical phase coexisting with a noncritical phase. The critical end points  $A$  and  $A'$  are special, since they coexist with each other;

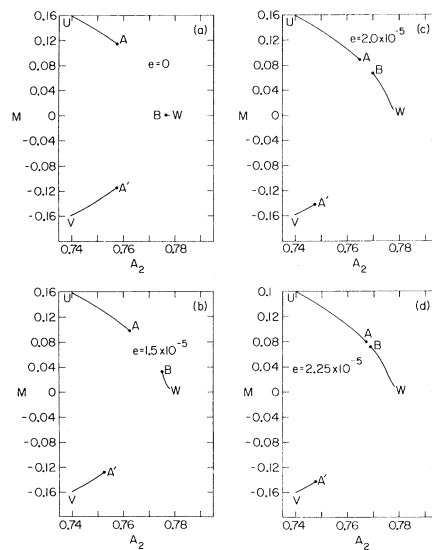


FIG. 7. Projection of a portion ( $A_2 \geq 0.74$ ) of the critical lines onto the  $M, A_2$ -plane. When (a)  $e = 0$ , the critical end points  $A$  and  $A'$  correspond to  $H = 0$ , and coexist with each other. The critical end point  $B$  corresponds to  $H = 0$ , and coexists with two noncritical phases. As  $e$  is increased to (b)  $e = 1.5 \times 10^{-5}$ , (c)  $e = 2.0 \times 10^{-5}$ , and (d)  $e = 2.25 \times 10^{-5}$ , the critical end points  $A$  and  $B$  approach one another. Eventually, they meet at the tricritical point. The point  $W$  corresponds to  $A_1 + A_2 + A_3 = 1$ .

hence each coexists with a critical phase. The symmetric critical line terminates in a critical end point marked  $B$ , which corresponds to  $H=0$  and  $M=0$ . It is also special, since at  $B$  a critical phase is coexisting with two noncritical phases. The nonsymmetric critical lines have been found by solving numerically Eqs. (2.22). The critical end points have been determined by finding all solutions of Eqs. (2.12) corresponding to the critical values of the fields, and then comparing the free energies  $\phi$  of each solution. The method used to solve (2.12) is discussed in Appendix B. It is instructive to compare Fig. 7(a) with Figs. 4(c) and 4(d), its analogue in the Landau theory.

Now, we consider  $e > 0$ . As  $e$  increases from zero, the critical end points  $A$  and  $B$  move toward each other. Where they meet is the nonsymmetric tricritical point. The projections of the critical lines corresponding to  $e = 1.5 \times 10^{-5}$ ,  $2.0 \times 10^{-5}$ , and  $2.25 \times 10^{-5}$  are shown, respectively, in Figs. 7(b), 7(c), and 7(d). The critical end points now correspond to a critical phase in equilibrium with one noncritical phase. We see the critical end points  $A$  and  $B$  have almost met for  $e = 2.25 \times 10^{-5}$ . For slightly larger values of  $e$ , there exists only one continuous line for  $M > 0$ . The only critical end point remaining would be  $A'$ , corresponding to  $M < 0$ .

#### V. CORRESPONDENCE BETWEEN SPIN-3/2 MODEL AND THE SYSTEM ETHANOL-WATER-CARBON-DIOXIDE

We consider the lattice-gas model of ternary fluid mixtures defined by the Hamiltonian (2.2), with the restricted form of the interactions specified by (2.3). We fix the interaction energies at the constant values  $E_0 = 1.2$ ,  $E_1 = 1 + e$ ,  $E_2 = -0.613$ ,  $E_3 = 1 - e$ , and  $e = 2.25 \times 10^{-5}$ . The thermodynamic variables may be taken to be the inverse temperature  $\beta$  and the densities  $A_1$ ,  $A_2$ , and  $A_3$ . The discussion of Sec. IV assures the existence of an isolated nonsymmetric tricritical point in the four-dimensional  $\beta, A$  space, with the tricritical temperature approximately given by  $\beta \approx 9$ . The explicit values of the interaction energies listed above are neither unique nor optimal. We are going to study one typical point on a four-dimensional surface of tricritical points, in the eight-dimensional  $E, \beta, A$  space.

Below the tricritical temperature, there exist two lines (in the four-dimensional  $\beta, A$  space) of critical end points, meeting at the tricritical point. For selected points along these lines, we present (Table II) the values of  $\beta$ ,  $A_1$ ,  $A_2$ ,  $A_3$ , and pressure  $p \equiv -\phi$ , corresponding to the critical and coexisting phases. The entries in Table II were computed in the following manner. Leaving  $\beta$  fixed, we varied  $A_2$  in steps of magnitude  $|\Delta| = 0.00025$ , and solved Eqs. (2.22) for the corresponding criti-

TABLE II. Densities  $A_1$ ,  $A_2$ ,  $A_3$  and the pressure  $p \equiv -\phi$  corresponding to inverse temperature  $\beta$  for the critical phase CEP(I) and the coexisting noncritical phase CX(I), and the critical phase CEP(II) and the coexisting noncritical phase CX(II). A rough estimate of the numerical uncertainties is given by  $\pm 1\%$  for  $A_1$  and  $A_3$  in critical phases, while  $A_2$  has only round-off error; and  $\pm 2\%$  for  $A_1$ ,  $A_2$ , and  $A_3$  in noncritical phases.

$\beta$	$A_1$	$A_2$	$A_3$	$p \equiv -\phi$
Critical end point [CEP(I)]				
9.0050	0.174	0.759	0.065	0.327292
9.0010	0.162	0.765	0.072	0.325683
9.0004	0.159	0.766	0.074	0.325451
9.0001	0.156	0.767	0.076	0.3253356
Coexisting phase [CX(I)]				
9.0050	0.115	0.777	0.107	0.327292
9.0010	0.136	0.773	0.089	0.325683
9.0004	0.139	0.772	0.087	0.325451
9.0001	0.144	0.771	0.084	0.3253356
Critical end point [CEP(II)]				
9.0050	0.135	0.774	0.090	0.327240
9.0010	0.145	0.771	0.083	0.325676
9.0004	0.147	0.770	0.081	0.325448
9.0001	0.149	0.770	0.080	0.3253351
Coexisting phase [CX(II)]				
9.0050	0.194	0.749	0.056	0.327240
9.0010	0.173	0.760	0.066	0.325676
9.0004	0.165	0.763	0.070	0.325448
9.0001	0.161	0.765	0.073	0.3253351

cal values of  $A_1$  and  $A_3$ . This determined critical lines in the three-dimensional  $A$  space. The stability of each critical point  $P(A_2)$  along these lines was checked by finding all solutions of Eqs. (2.12) corresponding to the critical values of the fields. In practice, we usually found that a critical end point lay between a point  $P(A_2)$  such that (2.12) had only the one critical solution, and a point  $P(A_2 + \Delta)$  such that (2.12) had three solutions, a noncritical solution being stable. The parameters describing the critical end point were approximated by the average of the critical parameters corresponding to  $P(A_2)$  and  $P(A_2 + \Delta)$ . The densities corresponding to the coexisting noncritical phase were less accurately determined. First, they had to be determined from the solution of (2.12), while the critical densities could be more directly determined by averaging two solutions of (2.22). Also, the uncertainties in the noncritical parameters were harder to estimate, because the noncritical phase usually did not appear before it was the stable solution of (2.12).

Shvarts and Efremova<sup>7</sup> have observed the two lines of critical end points meeting at the tricritical point in ethanol-water-carbon-dioxide mixtures.

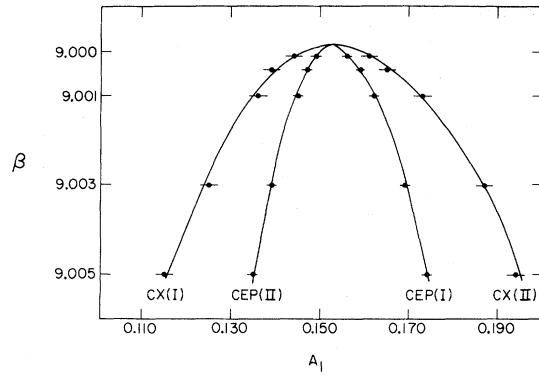


FIG. 8. Density  $A_1$  plotted against the inverse temperature  $\beta$ , for the critical phase CEP(I) and coexisting noncritical phase CX(I), and the critical phase CEP(II) and coexisting noncritical phase CX(II). Error bars indicate rough estimate of uncertainties in the numerical calculations.

They estimated the tricritical molar fractions to be  $N(\text{C}_2\text{H}_5\text{OH}) = 0.15$ ,  $N(\text{CO}_2) = 0.83$ , and  $N(\text{H}_2\text{O}) = 0.02$ . In our lattice-gas model, the molar fractions of the  $\lambda$ -type molecules is given by  $N(\lambda) = A_\lambda / (A_1 + A_2 + A_3)$ . From Table II, we see that  $A_0 = 1 - A_1 - A_2 - A_3 \approx 10^{-3}$ ; so  $N(\lambda) \approx A_\lambda$  is a good approximation. Comparing the table of Shvarts and Efremova<sup>7</sup> to Table II, we make the correspondence

- 1-type molecules  $\leftrightarrow$   $\text{C}_2\text{H}_5\text{OH}$ ,
- 2-type molecules  $\leftrightarrow$   $\text{CO}_2$ ,
- 3-type molecules  $\leftrightarrow$   $\text{H}_2\text{O}$ .

Carrying the correspondence further, we identify

- CEP(I): critical phase in liquid-liquid equilibrium;
- CX(I): gas phase coexisting with the liquid-liquid critical phase;
- CEP(II): critical phase in liquid-gas equilibrium;
- CX(II): heavy liquid phase coexisting with the liquid-gas critical phase.

In Fig. 8, we plot the temperature-ethanol mole-fraction ( $A_1$ ) curve, and find qualitative agreement with the corresponding Fig. 2 of Shvarts and Efremova.<sup>7</sup> The projection of the critical-end-point lines onto the temperature-pressure plane is given in Fig. 9. There is a qualitative difference between this figure and the analogous Fig. 1 of Shvarts and Efremova.<sup>7</sup> In the ethanol-water-carbon-dioxide system, the tricritical point lies at the maximum temperature and pressure. In our lattice-gas, the tricritical point lies at the maximum temperature, but the minimum pressure.

#### ACKNOWLEDGMENTS

We wish to thank Professor M. Blume for stimulating our interest in tricritical phenomena, and Professor V. J. Emery and Dr. D. Furman for interesting discussions. We also profited from two very clarifying discussions with Professor R. B. Griffiths.

#### APPENDIX A: PROOF OF EQ. (2.6)

We prove that the conditions

$$E_\lambda + E_\sigma > 0, \quad \lambda \neq \sigma = 0, 1, 2, 3, \quad (\text{A1})$$

are necessary and sufficient to rule out staggered order at zero temperature for all values of the chemical potentials. There are four types of translationally invariant orderings at  $T=0$ , corresponding to  $A_\lambda = 1$  ( $\lambda = 0, 1, 2, 3$ ). The energy per site associated with each type of ordering is given by Eqs. (2.2) and (2.3),

$$\tilde{E}(\lambda) = -\frac{1}{2}(E_\lambda + E_0) - \mu_\lambda \quad (\lambda = 1, 2, 3), \quad (\text{A2})$$

$$\tilde{E}(0) = 0.$$

The energy per site of a staggered ordering of molecules of types  $\lambda$  and  $\sigma$  is given by

$$\begin{aligned} \tilde{E}(\lambda, \sigma) &= -\frac{1}{2}E_0 - \frac{1}{2}(\mu_\lambda + \mu_\sigma), \quad (\lambda, \sigma \neq 0), \\ \tilde{E}(0, \lambda) &= -\frac{1}{2}\mu_\lambda. \end{aligned} \quad (\text{A3})$$

Suppose now that the ground state is translationally invariant for all values of the chemical potentials. We shall show that  $E_\lambda + E_\sigma > 0$ . Consider a value of the chemical potentials such that the ground

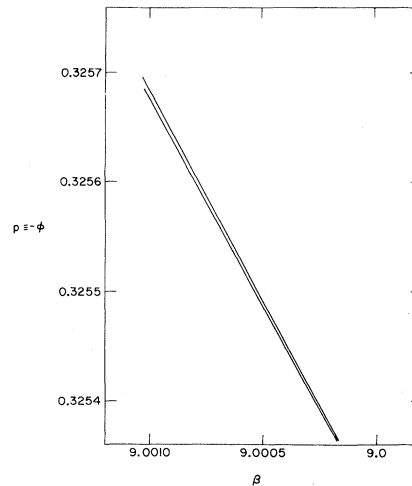


FIG. 9. Projection of critical end point lines onto pressure  $p \equiv -\phi$ , inverse temperature  $\beta$  plane. Tricritical point will lie at maximum temperature and minimum pressure. This is in contrast to experimental observations, which show tricritical point to lie at maximum temperature and maximum pressure.

state is  $A_\lambda = 1$ , and it is degenerate with  $A_\sigma = 1$ . For these values of the chemical potentials one has

$$\bar{E}(\lambda, \sigma) > \frac{1}{2} [\bar{E}(\lambda) + \bar{E}(\sigma)], \quad (\text{A4})$$

which implies [by using Eqs. (A2) and (A3)]  $E_\lambda + E_\sigma > 0$ .

On the other hand, if  $E_\lambda + E_\sigma > 0$ , then using Eqs. (A2) and (A3) one obtains

$$\bar{E}(\lambda, \sigma) > \frac{1}{2} [\bar{E}(\lambda) + \bar{E}(\sigma)], \quad (\text{A5})$$

for all values of the chemical potentials. This means that either  $\bar{E}(\lambda) < \bar{E}(\lambda, \sigma)$ , or  $\bar{E}(\sigma) < \bar{E}(\lambda, \sigma)$ , and the staggered order is not the ground state.

#### APPENDIX B: ANALYSIS OF EQS. (2.12)

In order to check the stability of a local minimum of  $\phi$ , it is necessary to determine all of the solutions of Eqs. (2.12) corresponding to the given values of the fields. We shall reduce the problem of solving the three simultaneous equations (2.12) to that of solving one equation in one unknown. It is then straightforward to numerically determine all of the solutions of this single equation. To proceed, note that (2.12) implies

$$A_2 = A_1 e^{\beta(\mu_2 - \mu_1 - E_1 A_1)} e^{\beta E_2 A_2},$$

$$A_3 = A_1 e^{\beta(\mu_3 - \mu_1 - E_1 A_1)} e^{\beta E_3 A_3}.$$

We implicitly define the function  $y = f(x)$  by  $y = x e^y$ . We introduce the notation

$$x_2 = \beta E_2 A_1 e^{\beta(\mu_2 - \mu_1 - E_1 A_1)},$$

$$x_3 = \beta E_3 A_1 e^{\beta(\mu_3 - \mu_1 - E_1 A_1)}.$$

It is now clear that the three equations (2.12) can

$$D = d^{-1} \begin{pmatrix} \alpha_0(\alpha_2 + \alpha_3) + \alpha_2 \alpha_3 & -\alpha_0 \alpha_3 & -\alpha_0 \alpha_2 \\ -\alpha_0 \alpha_3 & \alpha_0(\alpha_1 + \alpha_3) + \alpha_1 \alpha_3 & -\alpha_0 \alpha_1 \\ -\alpha_0 \alpha_2 & -\alpha_0 \alpha_1 & \alpha_0(\alpha_1 + \alpha_2) + \alpha_1 \alpha_2 \end{pmatrix}$$

Recall that the  $\alpha$ 's were defined in (2.14).

be replaced by the single equation in the one unknown  $A_1$ ,

$$\mu_1 = -(E_0 + E_1)A_1 - E_0 \left( \frac{f(x_2)}{\beta E_2} + \frac{f(x_3)}{\beta E_3} \right) + \beta^{-1} \ln \left( \frac{A_1}{1 - A_1 - f(x_2)/\beta E_2 - f(x_3)/\beta E_3} \right).$$

Once  $A_1$  is found from this equation, then

$$A_2 = f(x_2)/\beta E_2,$$

$$A_3 = f(x_3)/\beta E_3.$$

The function  $f(x)$  appearing in the above equations is double valued. We search for solutions corresponding to each of the four possible choices of branches. Even for a given choice of branches there are, in general, several solutions. The stable solution is the one which corresponds to the minimum value of the free energy  $\phi$ .

From (2.12), we can determine the susceptibility matrix

$$D \equiv \begin{pmatrix} \left. \frac{\partial A_1}{\partial \mu_1} \right|_{\mu_2 \mu_3} & \left. \frac{\partial A_1}{\partial \mu_2} \right|_{\mu_1 \mu_3} & \left. \frac{\partial A_1}{\partial \mu_3} \right|_{\mu_1 \mu_2} \\ \left. \frac{\partial A_2}{\partial \mu_1} \right|_{\mu_2 \mu_3} & \left. \frac{\partial A_2}{\partial \mu_2} \right|_{\mu_1 \mu_3} & \left. \frac{\partial A_2}{\partial \mu_3} \right|_{\mu_1 \mu_2} \\ \left. \frac{\partial A_3}{\partial \mu_1} \right|_{\mu_2 \mu_3} & \left. \frac{\partial A_3}{\partial \mu_2} \right|_{\mu_1 \mu_3} & \left. \frac{\partial A_3}{\partial \mu_3} \right|_{\mu_1 \mu_2} \end{pmatrix}.$$

Letting  $d$  denote the Jacobian given in (2.15),

$$d = \alpha_0 \alpha_1 \alpha_2 + \alpha_0 \alpha_2 \alpha_3 + \alpha_0 \alpha_3 \alpha_1 + \alpha_1 \alpha_2 \alpha_3,$$

we find

\*Work performed under the auspices of the U. S. Atomic Energy Commission.

<sup>1</sup>M. Blume, V. J. Emery, and R. B. Griffiths, Phys. Rev. A **4**, 1071 (1971).

<sup>2</sup>R. B. Griffiths, Phys. Rev. Lett. **24**, 715 (1970).

<sup>3</sup>R. B. Griffiths, J. Chem. Phys. **60**, 195 (1974).

<sup>4</sup>G. Stell and P. C. Hemmer, J. Chem. Phys. **56**, 4274 (1972).

<sup>5</sup>W. K. Theumann and J. S. Hoye, J. Chem. Phys. **55**, 4159 (1971).

<sup>6</sup>B. Widom, J. Phys. Chem. **77**, 2196 (1973).

<sup>7</sup>A. V. Shvarts and G. D. Efremova, Russ. J. Phys. Chem. **44**, 614 (1970).

<sup>8</sup>D. Mukamel and M. Blume, Phys. Rev. A **10**, 610 (1974); see also, J. Sivardière and J. Lajzerowicz (unpublished).

<sup>9</sup>J. Sivardière and M. Blume, Phys. Rev. B **5**, 1126 (1972).

<sup>10</sup>See, e.g., R. B. Griffiths, J. Math. Phys. **5**, 1215 (1964); H. Falk, Am. J. Phys. **38**, 858 (1970).

<sup>11</sup>If there is a double zero, no single direction is defined. In place of (2.17), one would obtain an expansion analogous to a Landau expansion in two order parameters.

<sup>12</sup>L. D. Landau and E. M. Lifshitz, *Statistical Physics*, 2nd ed. (Pergamon, London, 1969), Chap. 14.

<sup>13</sup>L. S. Schulman, Phys. Rev. B **7**, 1960 (1973).